ADDITIONAL INFRASONIC STUDIES OF EARTHQUAKES AND MINING BLASTS DISCRIMINATION

Douglas O. ReVelle

Los Alamos National Laboratory

Sponsored by National Nuclear Security Administration
Office of Nonproliferation Research and Engineering
Office of Defense Nuclear Nonproliferation

Contract No. W-7405-ENG-36

ABSTRACT

We have continued to examine earthquake and mining blast data to search for infrasonic detections using Los Alamos (LANL) infrasound arrays. During this past year, we examined all of the remaining earthquakes that were located at regional-scale, great-circle distances (< 1500 km) from the LANL DLIAR array. Once again, we have determined that about one of every nine earthquakes (generally between local seismic magnitudes 3 and 4) were detectable infrasonically. Although both stratospheric and thermospheric returns were generally evident, > ~58 % of all earthquakes or > ~ 55 % for all mining blasts only had thermospheric returns. The goal of this research is to be able to distinguish between earthquakes and small mining blasts using discriminants established using either infrasound or in conjunction with seismic data. The proposed discriminants include (1) amplitude correction for range (normalized) and amplitude-corrected for Stratospheric wind speed effects, but without application of these wind speed effects for thermospheric arrivals, (2) fast Fourier transform (FFT) power spectral analysis differences, (3) seismic R_g phases, i.e., as a fundamental depth discriminant over short propagation ranges.

OBJECTIVE

We will present the results of our analyses of earthquake-generated infrasonic signals from mining blast explosions. In this follow-up study, we will focus attention only on regional detections of small earthquakes and mining blasts (with local seismic magnitudes generally < 4 at ranges < 1500 km). The ultimate goal in this work is to establish reliable discriminants for distinguishing earthquakes from mining blasts for infrasonic and seismic detections made over regional propagation distances.

RESEARCH ACCOMPLISHED

A study of small earthquakes and small mining blasts was undertaken as an extension of last year's initial work on this subject. The latter study is still a work in progress, but will be briefly summarized. Data for the location and times of small earthquakes and mining blasts in the western US from 2000 to 2002 were assembled with the help of Professor B. Stump (SMU, Dallas, TX) and from a United States Geological Survey (USGS) website. Over 300 earthquakes and over 425 mining blasts were assembled for a subsequent infrasonic search for coherent signals with the requisite great-circle back azimuth, signal velocity and amplitude in order to be designated as having been detected at a single array. For mining blasts we demanded a much closer agreement between observations and processed data than we did for the small earthquakes. Because other researchers have shown that the epicenter need not be the source of the strongest infrasonic waves, we chose to use a weaker azimuth constraint on the deduced infrasound back azimuth from earthquakes (Le Pichon et al., 2003). The great-circle back azimuth deviations and all key associated parameters for the infrasonically detected earthquakes are summarized in Table 1. They are all generally < ~20° (but with one event ~34.5° away from the great-circle azimuth), fully consistent with previous studies for the larger earthquakes (ReVelle et al., 2004, Mutschlecner and Whitaker, 2005). Similarly, this information is listed for the mining blast shots in Table 2, where it can be observed that the great-circle azimuth deviations are usually much smaller, < ~5°, with a few exceptions. All infrasonic amplitudes and standard deviations listed have been revised from our single-channel analyses done last year. Amplitudes (in Pa) are generally averages of all four-signal channels within the 0.5 to 3-Hz passband. Occasionally, only three data channels were available, and these averages have been reported if they were deemed reliable. Amplitudes are also reported for each infrasonic return (phase). The various phases considered are listed in the footnotes in each of the two tables.

The new study emphasized regional-scale detection of small earthquakes and mining blasts, while the earlier study emphasized regional and teleseismic detection of much larger earthquakes. In order to proceed with the domain of very small sources, we wanted to establish a set of reasonable search criteria. Thus our new emphasis was to use the larger earthquakes as a guide for the successful detection of smaller events.

The approach used in our semiautomatic "nominal" data processing analysis for small events was to set various single-array selection criteria as follows (for infrasound signals whose duration above the prevailing background noise level was > 30-45 seconds, that were nominally band-pass filtered from 0.5 to 3.0 Hz using a Butterworth filter of order 2, initially for 20-s Hanning data windows with 50 % overlap between windows on a standard slowness plane consisting of 61 × 61 points):

i) A minimum cross-correlation threshold for > 3 consecutive data windows was set: $r_{min}^2 = 0.50$.

ii) A specific limit of allowable array trace speeds, V_{trace}: $0.28 \le V_{trace} \le 0.75$ km/sec. Equivalent slowness limits, S, in middle latitudes: 200 sec/degree ≤ S ≤ 400 sec/degree.

iii) A specific limit of allowable observed signal velocities, V_{sig} : $0.14 \le V_{sig} \le 0.36$ km/sec.

iv) A maximum deviation of the great-circle back azimuth from source to observer was set. This value was ± 25° for earthquakes and ± 5° for mining blasts for regional distances <1500 km.

v) Observed microbarom back azimuths were also determined for all events in order to be confident that the observed signals were not microbarom related "bursts" (< ~15 % of the final detections were removed because of this added constraint). With this effort a new microbarom identification/location tool, MCBAROM, was designed to reliably determine any

changes in the relevant back azimuths and speeds of microbaroms over about a 10-minute time window throughout the periods of interest (typically data blocks of one hour were used).

In MCBAROM, the plane wave, great-circle back azimuth was initially determined (for a data processing window duration of 500 seconds for a one-hour data interval) by first isolating the very stable long-period side of the microbarom band (using upper and lower frequencies of 0.150 and 0.125 Hz respectively). This allowed great-circle back azimuths to be determined that were generally in good agreement in middle latitudes with seasonally averaged wind speeds, i.e., easterly in summer and westerly in winter, etc. (Donn and Rind, 1972). Next, using the approach of Rind and Donn (1975), we were able to compute the stratospheric wind speed (temporally and spatially averaged values at an average height of ~50 km) by assuming a geometrical acoustics approach that relied on the constancy of the characteristic velocity generated at the source for a horizontally stratified, range-independent, steady-state atmosphere. In addition, by limiting microbarom trace velocities to values < ~ 0.50 km/s, we were successfully able to separate thermospheric microbarom arrivals from the desired stratospheric type. Assuming a sound speed at the turning height (from a model or direct observations), regular determinations of the wind speed at the turning height are possible from knowledge of the trace velocity of the microbaroms (Rind and Donn, 1975).

In all cases where detections were declared, a comparison was made between the Matseis/InfraTool, plane-wave, great-circle back azimuth and standard seismic f-k (frequency wavenumber) slowness plane approach in order to confirm all of our detections that were made using InfraTool. In addition, examinations of the spectrograms (frequency versus time as a function of acoustic power) often allowed an independent confirmation of the detections if the signal time period was not too "noisy."

After a semiautomatic detection was established for the searched events, either the data window size and/or the degree of overlap between data windows or the upper and lower band-pass frequency limits were systematically varied in order to refine the search. This approach took substantial amounts of time and needs to be automated, especially as the degree of overlap between data windows approaches large values.

So far in our data processing search, we have examined ~183 earthquakes and ~55 mining blasts using only the LANL array, DLIAR. Histogram distributions of the number of events versus local seismic magnitude and the number of events versus source-observer range for both earthquakes and mining blasts are plotted in Figures 1a to 1d. Of these 183 earthquakes, a total of 20 infrasonic detections were made with a high degree of certainty, while for the mining blasts a total of 16 high quality detections were made from a search of ~55 events in a similar local seismic magnitude range. Figure 2a illustrates infrasonic detection is illustrated of a small, shallow earthquake (# 102) that occurred on 12/01/2000 (local seismic magnitude 3.0, depth = 6.0 km). The corresponding MCBAROM tool results for the plane wave, back azimuth of microbaroms during this time interval are plotted in Figure 2b. The corresponding standard seismic f-k analysis for this infrasonic earthquake detection yielded a back azimuth of 270 ° (compared to 269 ° from InfraTool) with a corresponding slowness of 320 sec/deg.

A geographic summary of these infrasonic detections is given in Figure 3 where it is noted that for earthquakes, a repetition of source locations is clearly evident (in Idaho and in the CA-Baja region for example). In Figure 3, we have plotted the locations of both types of sources that we have detected at the DLIAR array as well as the locations of the other LANL infrasound arrays in the western US (with the exception of the Pinedale array at the Pinedale Seismic Research station in Wyoming). It can also be seen in Figure 3 that we may have the chance to detect these same sources at more than one infrasound array, a task which we will attempt after all events in our 2000-2002 database have been initially examined at DLIAR. Part of the reason for our success in detecting small mining blast relative to earthquakes is a result of the source ground-coupling factor and also the fact that the mining blast source is very near the Earth's surface. Earthquakes have two fundamentally different faulting mechanisms, only one of which is expected to generate significant infrasonic signals. In addition however, earthquake sources can also be at great depths. Since the generation of infrasound is fundamentally related to the up-down part of the source ground motion, deeper earthquakes are generally not expected to generate significant infrasound. The deepest source that has been detected infrasonically so far was 13.8 km, while others were detected closer

to the earth's surface. Eventually we will examine all of our infrasonic earthquake detections in terms of both their depth and faulting mechanisms, etc.

We also examined our detections in terms of establishing possible discriminants between small mining blast and earthquakes. We are currently examining earlier predictions of wind-corrected infrasonic amplitude versus local seismic magnitudes that were developed for larger sources at generally longer ranges to determine if we can establish a similar regression curve for use in the small source-size range. Additional discriminants currently being investigated include the following:

i) Separate analyses of the relationship between infrasonic amplitudes from earthquakes and from mining blasts (as normalized for range and corrected for stratospheric wind effects) versus the local seismic magnitude have been made. In the case of thermospheric arrivals, wind corrections are not made; however, because for such returns wind speeds are generally << than the local sound speed at such large heights and do not limit the ducting possibilities.
ii) PSD (power spectral density) analysis of differences between earthquakes and mining blasts.
iii) Seismic R_g phases for separating earthquake signals from mining blasts over short-range shallow propagation paths, i.e., as a fundamental depth-discriminant concept.

In the coming year, we will continue to pursue all of these activities and develop a conceptual framework for the reliable discrimination of infrasonic signals from earthquakes from those from mining blasts.

CONCLUSIONS AND RECOMMENDATIONS

We have examined a fairly wide range of small earthquake and mining blast magnitudes and distances. For large earthquakes, we previously determined that a relationship exists between the wind-corrected and range-normalized infrasonic amplitude and the local seismic magnitude, and we wish to determine if this relationship is still applicable for smaller magnitude sources. If a similar regression line can be established for small sources over regional detection distances, at least one physical discriminant can be readily developed for separating mining blast shots from earthquakes. This discrimination tool will be a very important development since a very large number of both types of sources occur annually worldwide. Our general conclusions at this time for the current set of processed results are the following:

1) Durations of earthquakes are generally much larger than those of the mining blast shots, with the exception of the mining blast shot at Newcastle, Wyoming on 2/26/2001 (total duration > 4 min).
2) The earthquake detections are generally "cleaner," i.e., the standard deviation of the recorded amplitudes averaged over all available data channels, is generally much smaller with respect to the average value.
3) Our concentration of work efforts next year will be entirely on mining blast shots and this should help to clarify the current situation and further our efforts to reliably discriminate between these source types.

REFERENCES

Donn, W. L. and D. Rind (1972), Microbaroms and the temperature and wind of the upper atmosphere, *J. Atmos. Sci*. 29, 156-172.

Le Pichon, A., M. Aupetit, E. Blanc, Y. Cansi, J. Guilbert, S. Lambotte and J. Plantet (2003), Six-years review of infrasound monitoring at the French NDC, Invited Abstract U32C-01, American Geophysical Union Annual Fall Meeting, San Francisco.

Mutschlecner, J. P. and R. W. Whitaker (2005), Infrasound from earthquakes, *J. Geophys. Res*. 110: D01108.

ReVelle, D. O., R. W. Whitaker, J. P. Mutschlecner and M. Renwald (2004), Discrimination of earthquakes and mining blasts using infrasound, in *Proceedings of the 26th Seismic Research Review—Trends in Nuclear Explosion Monitoring*, LA-UR-04-5801, Vol. 2, pp. 669-679.

Rind, D. and W. L. Donn (1975), Further use of natural infrasound as a continuous monitor of the upper atmosphere, *J. Atmos. Sci*. 32: 1694-1704.

Webb, W. L. (1964), Stratospheric solar response, *J. Atmos. Sci*. 21: 582-591.

Young, H.D. (1962), *Statistical Treatment of Experimental Data,* McGraw-Hill Book Co., Inc., 172 pp.

Table 1: Summary: Regional Scale Earthquake Detections- DLIAR infrasound array (*)

Earth-quake	Date: mm/dd/yy	General Location	Time: UT	Local Seismic magnitude and depth: km	Range km- along great circle path	G.C. (**) back azimuth: (BA): °	ΔBA: (***): °	Raw amp. Pa: 4 channel average value ± stand. dev.	Signal velocity: km/s and phase type(s) (*****)
# 17	2/29/00	CA-NV	22:08	4.1, 0.0	1013.2	268.0	3.5 -7.5	0.032 ±0.012 0.014 ±0.006	0.32, S 0.24, Th
# 42/44	5/26/00	WY	21:58	4.0, 5.0	711.8	351.0	-3.8	0.092 ±0.018	0.22, Th
# 85	11/10/00	MT	19:14	4.0, 2.1	1243.9	338.5	10.1 -12.5	0.038 ±0.014 0.025 ±0.015	0.28, S 0.14, Slow Th
# 102	12/01b/00	S. NV	00:01	3.0, 6.0	778.2	269.0	-2.7 -6.2	0.014 ±0.004 0.009 ±0.003	0.29, S 0.20, Th
# 177	9/04/01	CO	12:45	4.0, 5.0	206.9	47.2	2.2	0.031 ±0.002	0.29, S
# 191	10/08a/01	E. Idaho	13:47	3.6, 0.1	1140.4	328.9	2.6 34.5 (??)	0.007 ±0.001 0.055 ±0.004 (??)	0.28, S 0.14, Slow Th
# 192	10/08b/01	NV	05:37	4.6, 0.0	1018.4	302.7	12.7	0.008 ±0.003	0.22 Th
# 206	12/09/01	W. AZ-Sonora	01:42	4.5, 10.0	901.8	239.7	-2.7	0.026 ±0.007	0.26 Th
# 207	12/12/01	MT	11:17	3.0, 5.6	1122.3	333.9	3.0	0.013 ±0.002	0.22, Th
# 208	12/13/01	W. Idaho	05:42	3.2, 5.0	1251.5	323.0	-6.4 -13.8	0.020 ±0.009 0.013 ±0.003	0.31, S 0.25, Th
# 221	01/04e/02	CA-Baja	19:38	3.3, 7.0	885.4	242.9	21.3	0.079 ±0.012	0.31, S
# 222	01/04f/02	E. Idaho	13:11	3.2, 5.0	908.2	329.2	-8.0	0.007 ±0.002 (****)	0.16, Slow Th
# 225	01/08/02	UT	17:26	3.2, 8.2	592.1	281.1	1.8	0.046 ±0.006	0.20 Th
# 230	01/22/02	W. Idaho	08:31	3.7, 5.0	1160.8	322.5	16.7	0.015 ±0.002	0.30, S
# 239	02/22/02	CA-Baja	19:32	5.5, 7.0	916.3	242.0	-3.6	0.069 ±0.011	0.29, S
# 242	03/19/02	Gulf of CA	22:14	4.1, 10.0	935.3	225.0	-10.6	0.118 ±0.017	0.27, S
# 264	05/11/02	UT	06:30	3.0, 9.2	800.5	323.4	4.2	0.042 ±0.016	0.24, Th
# 265	05/14/02	Central CA	05:00	4.9, 7.7	1370.0	270.5	-16.4	0.052 ±0.004	0.14 Slow Th
# 278	07/15/02	CA-NV	20:18	4.1, 13.0	1089.7	275.3	-1.8 18.1	0.061 ±0.015 0.061 ±0.016	0.31, S 0.16, Slow Th
# 279	07/23/02	E. Idaho	08:17	3.0, 5.0	864.0	329.3	8.2	0.016 ±0.004	0.18, Slow Th

(*): Final regional earthquake detection list at DLIAR: All marginal detections have been removed. The removal of events was finally decided on the basis of too brief a signal duration, a back azimuth too close to the prevailing microbaroms back azimuth (available from MCBAROM), or too small an r^2 value, etc.

The amplitude computations were made using $\Delta p\ (Pa) = 0.5 \cdot \Delta S_{p\text{-}p}(cm) \cdot \{2.5\ Pa/V\} \cdot S(V/cm)$, where S is the scale factor for each individual microphone channel and $\Delta S_{p\text{-}p}$ is the individual channel maximum signal amplitude (peak-to-peak value). Symmetry of the total amplitude about the origin was assumed, so that the zero-to peak-value was calculated to be one half of the maximum total signal amplitude.

(**) InfraTool great-circle, back azimuth Towards the USGS source location from the DLIAR array.

(***) Plane-wave, back azimuth deviation from the great-circle path back to the infrasonic source

ΔBA = Computed great-circle back azimuth – observed standard seismic f-k back azimuth

(****) Marginal amplitude measurement at very low S/N ratio

(*****) Infrasonic phases are L: Lamb, T: Tropospheric, S: Stratospheric, Th: Thermospheric and Slow Th: Slow Thermospheric returns.

Table 2: Mining Blast Infrasound Detections Summary: (∗)

Mining blast shot location	Date mm/dd/yy	Time: UT	Local Seismic Magnitude	Range: km- along great-circle path	G.C. (∗∗), back azimuth (BA): °	Δ BA (∗∗∗): °	Raw amp. Pa: 4 channe average value ± stand. dev.	Signal velocity: km/s and Arrival phase type(s) (∗∗∗∗∗)
Newcastle,WY	2/26/01	21:09	3.5	871.0	7.9	0.80	0.027 ±0.013	0.28, S
Craig, CO	2/28b/01	23:06	3.3	510.7	344.8	16.4	0.010 ±0.006	0.34, L
Safford, AZ	3/22/01	19:19	3.2	417.2	221.2	1.4 -5.7	0.074 ±0.024 0.383 ±0.243 (??)	0.30, S 0.15, Slow Th
Gillette, WY	3/27/01	21:17	3.1	880.5	6.5	-2.3 -17.9 (∗∗∗∗)	0.054 ±0.013 0.029 ±0.012	0.35, L 0.17 Slow Th
Gillette, WY	4/01/01	20:10	3.1	880.5	6.5	6.5	0.022 ±0.005	0.32, S
Gillette,WY	4/25a/01	20:04	3.2	880.5	6.5	-3.4	0.025 ±0.016	0.31, S
Safford, AZ	4/25b/01	22:13	3.4	417.2	221.5	-3.8	0.015 ±0.007	0.28, S
Safford, AZ	4/30/01	18:50	3.1	417.2	221.5	-5.6 -20.6 (??)	0.017 ±0.013 0.024 ±0.016 (??)	0.25, Th 0.17, Slow Th
Gillette,WY	5/12/01	20:02	3.3	880.5	6.5	1.5	0.015 ±0.009	0.14, Slow Th
Sheridan,WY	6/19/01	19:03	3.1	1039.9	359.2	-0.80	0.037 ±0.022	0.32,T/S
Rock Springs,WY	6/26/01	21:38	3.2	674.9	341.9	7.3	0.012 ±0.005	0.22, Th
Craig, CO	6/27/01	18:14	3.5	510.7	344.8	1.3	0.090 ±0.040	0.14, Slow Th
Gillette, WY	7/04/01	18:18	3.4	880.5	6.5	-1.6	0.074 ±0.018	0.28, S
Craig, CO	7/07/01	22:04	3.5	510.7	344.8	-1.2	0.080 ±0.025	0.21, Th
Rock Springs,WY	7/11/01	17:16	3.3	674.9	341.9	-4.7	0.072 ±0.031	0.24, Th
Craig, CO	8/18/01	13:58	3.3	510.7	344.8	-2.9 -2.4	0.008 ±0.003 0.012 ±0.004 (?)	0.26, Th 0.11, Slow Th

(∗): This list is not final yet, since numerous mining blast shots still need to be evaluated infrasonically.

The amplitude computations were done using: $\Delta p\ (Pa) = 0.5 \cdot \Delta S_{p\text{-}p}(cm) \cdot \{2.5\ Pa/V\} \cdot S(V/cm)$ where S is the scale factor for each individual microphone channel and $\Delta S_{p\text{-}p}$ is the individual channel maximum signal amplitude (peak to peak value). Symmetry of the total amplitude about the origin was also assumed so that the zero to peak value was calculated to be one half of the maximum total signal amplitude.

(∗∗): Infra_Tool great-circle, back azimuth: Towards the USGS source location from the DLIAR array.

(∗∗∗): Plane wave, back azimuth deviation from the great-circle path back to the infrasonic source: ΔBA = Computed great-circle back azimuth – observed standard seismic f-k back azimuth

(∗∗∗∗): Using Infra_Tool's back azimuth for this Slow Th phase, Δ BA = 1.6 °. The reason for this discrepancy is not yet understood.

(∗∗∗∗∗) Infrasonic phases are L: lamb, T: tropospheric, S: stratospheric, Th: thermospheric and Slow Th: Slow thermospheric returns

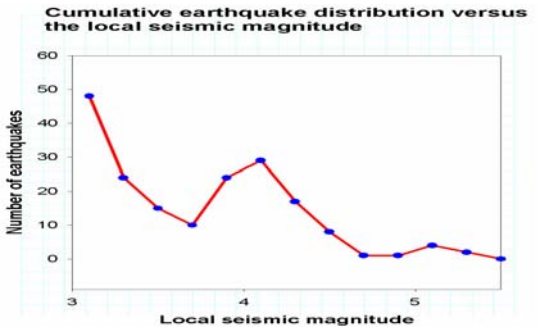

Figure 1a. Number of earthquakes versus local seismic magnitude.

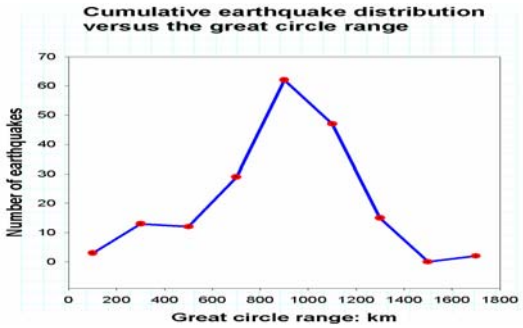

Figure 1b. Number of earthquakes versus source-observer range.

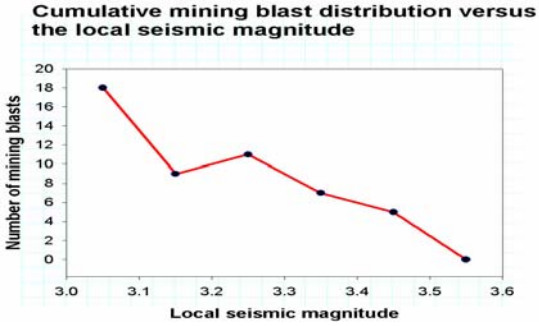

Figure 1c. Number of mining blasts versus local seismic magnitude.

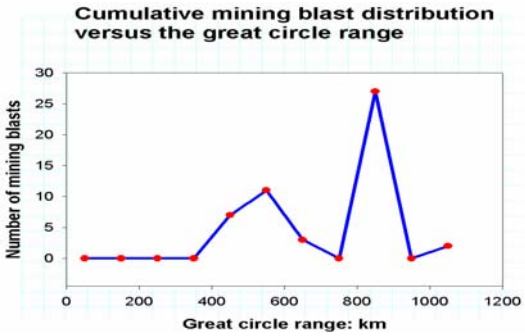

Figure 1d. Number of mining blasts versus source-observer range

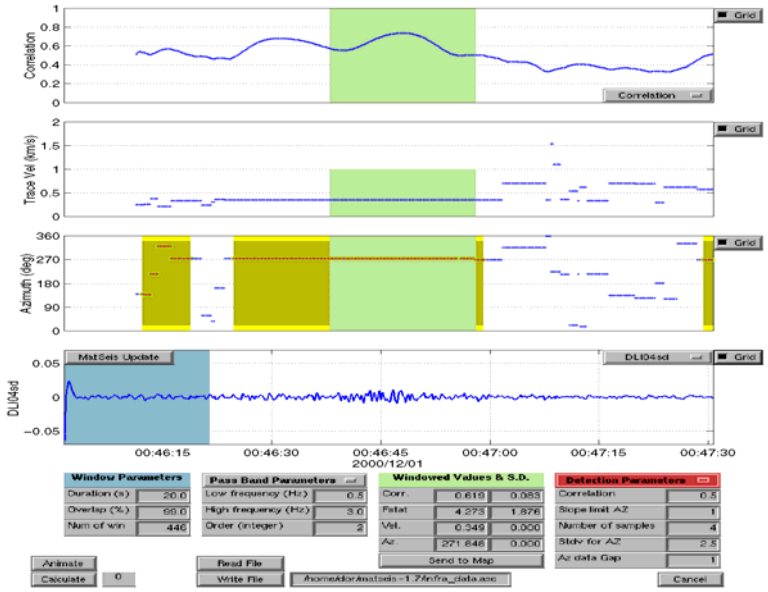

Figure 2a. Matseis signal processing and analysis: Infrasonic detection of earthquake (# 102) of 12/01b/2000. Averaged pair-wise cross-correlation, trace velocity, back azimuth, and a single-channel time series versus pressure amplitude.

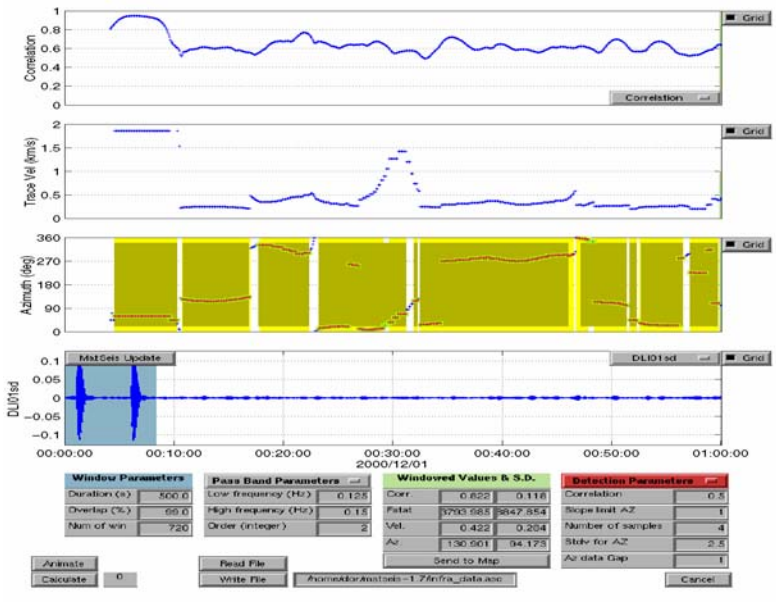

Figure 2b. Matseis signal processing and analysis: detection results during the same time interval as for earthquake (# 102) of 12/01b/2000 in Figure 1a. Averaged pair-wise cross-correlation, trace velocity, back azimuth, and a single-channel time series versus pressure amplitude.

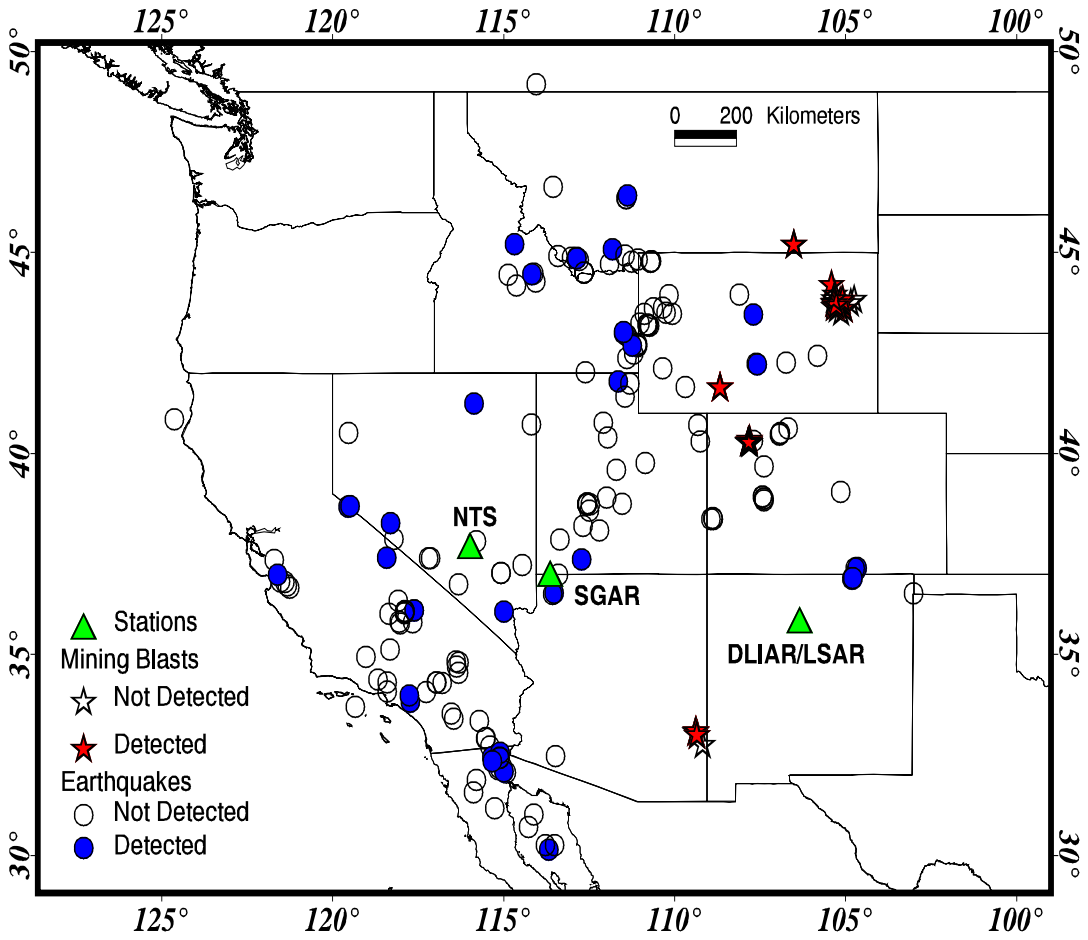

Figure 3. Spatial summary: infrasonic detections of small earthquakes and mining blasts.